Stochastic response analysis and optimization of a class of nonlinear electromechanical energy harvesters

Ioannis Petromichelakis[a], Apostolos F. Psaros[a], Ioannis A. Kougioumtzoglou[a,*]

[a] *Department of Civil Engineering and Engineering Mechanics, Columbia University, 500 W 120th St, New York, NY 10027, United States*

Abstract

A methodology based on the Wiener path integral technique (WPI) is developed for stochastic response determination and optimization of a class of nonlinear electromechanical energy harvesters. To this aim, first, the WPI technique is extended to address the particular form of the coupled electromechanical governing equations, which possess a singular diffusion matrix. Specifically, a constrained variational problem is formulated and solved for determining the joint response probability density function (PDF) of the nonlinear energy harvesters. Next, the herein extended WPI technique is coupled with an appropriate optimization algorithm for determining optimal energy harvester parameters. It is shown that due to the relatively high accuracy exhibited in determining the joint response PDF, the WPI technique is particularly well-suited for constrained optimization problems, where the constraint refers to low probability events (e.g. probabilities of failure). In this regard, the WPI technique outperforms significantly an alternative statistical linearization solution treatment commonly utilized in the literature, which fails to capture even basic features of the response PDF. This inadequacy of statistical linearization becomes even more prevalent in cases of nonlinear harvesters with asymmetric potentials, where the response PDF deviates significantly from the Gaussian. An illustrative example is considered, while comparisons with pertinent Monte Carlo simulation data demonstrate the robustness and reliability of the methodology.

Keywords: energy harvesting; path integral; stochastic dynamics; nonlinear system; optimization

1. Introduction

Vibratory energy harvesters [1] have flourished in recent years as an alternative to common energy sources such as batteries. The rationale behind this technology is that compact and scalable electronic devices can be powered by exploiting the ability of active materials (e.g. piezoelectric) to generate an electric potential in response to external excitation. A cantilever beam with piezoelectric patches attached near its clamped end is one of the most widely used energy harvesters [1]. The beam is subjected to environmental excitation causing large strains near the clamped end, thus producing a voltage difference across the patches, which is converted into electrical current by utilizing an appropriate circuit. Typically, energy harvesters have been modeled in the literature as linear systems designed by tuning the first natural frequency to achieve resonance with a given

*Corresponding author
Email address: ikougioum@columbia.edu (Ioannis A. Kougioumtzoglou)

a priori known deterministic (harmonic) excitation. To compensate for the significant reduction of the power output at off-resonant frequencies, researchers have considered designs with nonlinear restoring forces (e.g. proportional to the cube of the deflection), which are known to increase the effective resonance bandwidth of the harvester. Further, most energy harvesters operate in tandem with structures and civil infrastructure systems (e.g. bridges), which are subjected to environmental excitations that have random characteristics, and are thus most realistically modeled as stochastic processes [2].

In the harvester design process, besides the obvious criterion of maximum energy output, additional restrictions in terms of maximum displacement of the mechanical oscillator may be required in realistic situations due to limited available space, or to avoid potential mechanical failures. In this regard, constraints may often relate to the probability that the voltage and/or the displacement stay within prescribed limits, a strategy that can potentially lead to more robust and efficient designs than what is currently the norm in the literature. In this paper, a methodology for stochastic response determination and optimization of nonlinear energy harvesters is developed based on the Wiener path integral technique (WPI) [3, 4]. To this aim, first, the WPI technique is extended to account for the singular diffusion matrix related to the governing equations, by considering the electrical equation as a constraint, leading to a linearly constrained variational problem to be solved by nullspace [5] based approaches. Next, the herein extended WPI technique is coupled with an appropriate optimization algorithm for determining efficiently the harvester optimal parameters, accounting even for low probability events (e.g. failures) as constraints. An illustrative example is considered, while comparisons with pertinent Monte Carlo simulation (MCS) data demonstrate the robustness and reliability of the methodology.

2. Nonlinear electromechanical energy harvester

2.1. Modeling aspects

As discussed in detail in [1], the dynamics of the system modeling the cantilever beam energy harvester, can be approximated by the following general mathematical model of coupled electromechanical equations, expressed in a non-dimensional form as

$$\ddot{x} + 2\zeta\dot{x} + dU(x)/dx + \kappa^2 y = w(t) \tag{1a}$$

$$\dot{y} + \alpha y - \dot{x} = 0 \tag{1b}$$

where x = response displacement; y = electrical quantity (voltage or current); ζ = damping; κ = coupling coefficient; α = electrical constant; $U(x)$ = potential function and $w(t)$ = external excitation, which is modeled as a Gaussian white noise stochastic process. The derivative $dU(x)/dx$ represents the generally nonlinear restoring force which is assumed to be a 3^{rd} order polynomial of the displacement x and takes the non-dimensional form

$$dU(x)/dx = x + \lambda x^2 + \delta x^3 \tag{2}$$

where λ and δ control the intensity of the quadratic and cubic nonlinear terms, respectively. In the present paper, attention is restricted to monostable asymmetric harvesters, implying that $0 < \lambda \leq 2\sqrt{\delta}$ and $\delta > 0$. For this class of nonlinear energy harvesters, it has been argued that maximum mean harvested power is achieved for $\lambda = 2\sqrt{\delta}$ [6].

2.2. Optimization aspects

From an optimal design perspective, the objective is typically articulated in the literature as maximizing the mean stationary harvested power

$$P_h = \alpha \mathbb{E}\{y^2\} \tag{3}$$

for a given excitation intensity S_0; this can be formulated as an optimization problem. In this regard, the parameter ζ includes the mass, damping and stiffness coefficients of the mechanical system, and its value is dictated by physical constraints of the particular application, while κ has a monotonic effect on the harvested power. Accordingly, both ζ and κ are considered fixed and only the nonlinearity δ and the electrical constant α are being optimized.

In practice, it is often desirable to apply additional design criteria that enforce constraints related to the probability that y and/or x stay within prescribed limits. Such a constraint can take the general form $P_f < \epsilon$, where the probability of failure P_f is typically related to an "extreme event" characterized by a low probability of occurrence. In this regard, for the parameter vector $z = [\alpha, \delta]$ and for ζ, κ and S_0 fixed, the constrained optimization problem

$$\underset{\boldsymbol{z} \in Z}{\arg\max}\, P_h(\boldsymbol{z}) \quad \text{s.t.} \quad P_f(\boldsymbol{z}) \leq \epsilon \tag{4}$$

is formulated, where $Z \subset \mathbb{R}^2_{++}$ is an effective domain of parameter values, $\mathbb{R}_{++}$ denotes the set of positive real numbers and ϵ is a prescribed value.

Note, however, that a requirement for addressing this problem, is the complete stochastic characterization of the system response, i.e., knowledge of the joint response PDF, and not only of the response mean and variance. To this aim, the WPI response determination technique is extended and applied herein for addressing the constrained optimization problem of Eq. (4).

3. Wiener Path integral solution technique overview

One of the recently developed promising techniques in stochastic engineering dynamics, that exhibits relatively high accuracy in determining the joint response PDF, relates to the concept of the Wiener path integral (WPI) [3]. The essential aspects of the technique are delineated in the present section by considering the general class of n-dimensional randomly excited structural/mechanical systems whose dynamics is described by

$$\boldsymbol{D}[\boldsymbol{q}(t)] = \boldsymbol{w}(t) \tag{5}$$

where $\boldsymbol{D}[.]$ = nonlinear differential operator, $\boldsymbol{q}$ = system response, and $\boldsymbol{w}$ = a white noise stochastic excitation vector process with $E[\boldsymbol{w}(t_1)\boldsymbol{w}(t_2)] = \boldsymbol{B}\delta(t_2 - t_1)$; $\delta(.)$ denotes the Dirac delta function and $\boldsymbol{B}$ is the deterministic diagonal coefficient matrix with the value $2\pi S_0$ in the diagonal.

Next, the transition PDF $p(\boldsymbol{q}_f, \dot{\boldsymbol{q}}_f, t_f | \boldsymbol{q}_i, \dot{\boldsymbol{q}}_i, t_i)$ with $(\boldsymbol{q}_i, \dot{\boldsymbol{q}}_i, t_i)$ denoting the initial state and $(\boldsymbol{q}_f, \dot{\boldsymbol{q}}_f, t_f)$ the final state, and $\boldsymbol{q}_i = \boldsymbol{q}(t_i)$, $\boldsymbol{q}_f = \boldsymbol{q}(t_f)$, $\dot{\boldsymbol{q}}_i = \dot{\boldsymbol{q}}(t_i)$ and $\dot{\boldsymbol{q}}_f = \dot{\boldsymbol{q}}(t_f)$, can be written as [4]

$$p(\boldsymbol{q}_f, \dot{\boldsymbol{q}}_f, t_f | \boldsymbol{q}_i, \dot{\boldsymbol{q}}_i, t_i) = \int_{\mathcal{C}\{\boldsymbol{q}_i, \dot{\boldsymbol{q}}_i, t_i; \boldsymbol{q}_f, \dot{\boldsymbol{q}}_f, t_f\}} W[\boldsymbol{q}(t)][\mathrm{d}\boldsymbol{q}(t)] \tag{6}$$

The above integral represents a functional integration over the space of all possible paths $\mathcal{C}\{\boldsymbol{q}_i, \dot{\boldsymbol{q}}_i, t_i; \boldsymbol{q}_f, \dot{\boldsymbol{q}}_f, t_f\}$, $W[\boldsymbol{q}(t)]$ denotes the probability density functional of the stochastic process in the path space and $[\mathrm{d}\boldsymbol{q}(t)]$ is a functional measure. The probability density functional for the stochastic process $\boldsymbol{q}$ pertaining to the system of Eq. (5) is defined as $W[\boldsymbol{q}(t)] = \exp\Big(-\int_{t_i}^{t_f} \mathcal{L}\left(\boldsymbol{q}, \dot{\boldsymbol{q}}, \ddot{\boldsymbol{q}}\right) \mathrm{d}t\Big)$ where C is a normalization constant and $\mathcal{L}\left(\boldsymbol{q}, \dot{\boldsymbol{q}}, \ddot{\boldsymbol{q}}\right)$ is the Lagrangian of the MDOF system given by

$$\mathcal{L}(\boldsymbol{q}, \dot{\boldsymbol{q}}, \ddot{\boldsymbol{q}}) = \frac{1}{2}\boldsymbol{D}[\boldsymbol{q}]^T \boldsymbol{B}^{-1} \boldsymbol{D}[\boldsymbol{q}] \tag{7}$$

Clearly, the largest contribution to the aforementioned functional integral comes from the trajectory $\boldsymbol{q}_c(t)$ for which the integral in the exponential (also known as the stochastic action) becomes as small as possible. Variational calculus rules dictate that this trajectory with fixed endpoints satisfies the extremality condition $\delta \int_{t_i}^{t_f} \mathcal{L}(\boldsymbol{q}, \dot{\boldsymbol{q}}, \ddot{\boldsymbol{q}})\mathrm{d}t = 0$ which leads to the Euler-Lagrange (E-L) equations

$$\frac{\partial \mathcal{L}}{\partial q_j} - \frac{\partial}{\partial t}\frac{\partial \mathcal{L}}{\partial \dot{q}_j} + \frac{\partial^2}{\partial t^2}\frac{\partial \mathcal{L}}{\partial \ddot{q}_j} = 0, \quad j = 1, ..., n \tag{8}$$

with the set of $4 \times n$ boundary conditions

$$\begin{matrix} q_j(t_i) = q_{j,i} & \dot{q}_j(t_i) = \dot{q}_{j,i} \\ q_j(t_f) = q_{j,f} & \dot{q}_j(t_f) = \dot{q}_{j,f} \end{matrix} \qquad j = 1, ..., n \tag{9}$$

Next, solving equations (8)-(9) yields the n-dimensional most probable path, $\boldsymbol{q}_c(t)$, and thus, a single point of the system response transition PDF can be determined as [4]

$$p(\boldsymbol{q}_f, \dot{\boldsymbol{q}}_f, t_f | \boldsymbol{q}_i, \dot{\boldsymbol{q}}_i, t_i) \approx C \ \exp\left(-\int_{t_i}^{t_f} L(\boldsymbol{q}_c, \dot{\boldsymbol{q}}_c, \ddot{\boldsymbol{q}}_c)\mathrm{d}t\right) \tag{10}$$

where C is a normalization constant.

Further, note that instead of solving the derived E-L equations (8)-(9), an alternative, direct functional minimization formulation can be applied, which can be readily coupled with a standard Rayleigh-Ritz solution approach (see [7]) for determining the most probable path $\boldsymbol{q}_c(t)$. In this regard, $\boldsymbol{q}$ is approximated by

$$\hat{\boldsymbol{q}} = \boldsymbol{\psi} + \boldsymbol{R}\boldsymbol{h} \approx \boldsymbol{q}. \tag{11}$$

The function $\boldsymbol{\psi}(t)$ is chosen so that it satisfies the boundary conditions, while the trial functions $\boldsymbol{h}(t) = [h_0, h_1, ..., h_{L-1}]^T$ should vanish at the boundaries.. $\boldsymbol{R} \in \mathbb{R}^{n \times L}$ is a coefficient matrix, where L is the chosen number of trial functions considered. Clearly, there is a wide range of options for the choice of functions $\boldsymbol{\psi}$ and $\boldsymbol{h}$. In the ensuing analysis, the functions $\boldsymbol{\psi}$ take the form of the Hermite interpolating polynomials, while the trial functions $\boldsymbol{h}$ are defined with the aid of the shifted Legendre polynomials as in [8].

A practical advantage of the Rayleigh-Ritz method is that the variational problem (functional minimization) degenerates to an ordinary minimization problem of a function that depends on a finite number of variables [9]. Specifically, the functional $\mathcal{J}(\boldsymbol{q})$, dependent on the n functions $\boldsymbol{q}(t)$, is replaced by the function $J(\boldsymbol{R})$, dependent on a finite number of $n \times L$ coefficients $\boldsymbol{R}$. Accordingly, the extremality condition $\delta \int_{t_i}^{t_f} \mathcal{L}(\boldsymbol{q}, \dot{\boldsymbol{q}}, \ddot{\boldsymbol{q}})\mathrm{d}t = 0$ is replaced by $\frac{\partial J(\boldsymbol{R})}{\partial \boldsymbol{R}} = \boldsymbol{0}$ which represents essentially a set of nL nonlinear equations for the unknown coefficients (parameters) $\boldsymbol{R}$. Once solved numerically, the most probable path $\boldsymbol{q_c}$ is determined via Eq. (11).

4. Extension of the Wiener path integral technique to account for singular diffusion matrices: A constrained variational problem

Taking into account the form of Eq. (1), it can be readily seen that a straightforward application of Eq. (7) is not possible, as it would lead to a singular matrix $\boldsymbol{B}$. Thus, a modification is required to the WPI technique presented in Sec. 3 to account for the special form of Eq. (1). In this regard, consider Eq. (1a) as an under-determined stochastic differential equation (SDE) with 2 unknowns (x and y), excited by the Gaussian white noise process $w(t)$. For this SDE, and for $\boldsymbol{q} = [\alpha, \delta]^T$, the Lagrangian can be expressed as

$$\mathcal{L}(x, y, \dot{x}, \ddot{x}) = \frac{1}{4\pi S_0}\left[\ddot{x} + 2\zeta\dot{x} + x + 2\sqrt{\delta}x^2 + \delta x^3 + \kappa^2 y\right]^2 \tag{12}$$

Clearly, considering Eq. (12) alone is inadequate, as the dynamics described by Eq. (1b) have so far been neglected. To proceed, Eq. (1b) is treated next as a constraint in the form

$$\phi(y, \dot{y}, \dot{x}) = \dot{y} + \alpha y - \dot{x} = 0 \tag{13}$$

Eq. (12) in conjunction with Eq. (13) lead to a constrained variational problem, where the constraint function is linear with respect to x, y and $\dot{y}$. In this regard, adopting the Rayleigh-Ritz scheme of Sec. 3, and utilizing the polynomial expansion $\hat{\boldsymbol{q}} = \boldsymbol{\psi} + \boldsymbol{R}\boldsymbol{h}$ for $\boldsymbol{q}$ (see Eq. (11)), the constrained variational problem is formulated as a constrained optimization problem. Utilizing a nullspace approach next, the optimization is restricted within the space of solutions of $\phi(\hat{\boldsymbol{q}}, \dot{\hat{\boldsymbol{q}}}) = \hat{\phi}(t) = 0$.

Specifically, linearity of the constraint equation ensures that $\hat{\phi}(t)$ is a polynomial of degree $L + 4$ in t (see equations (11) and (13)), with coefficients linear in the $2L$ unknown expansion parameters $\boldsymbol{R} \in \mathbb{R}^{2\times L}$. Setting these polynomial coefficients equal to zero, yields a set of $L + 4$ linear equations with $2L$ unknown variables. Next, expressing the unknown parameters $\boldsymbol{R} \in \mathbb{R}^{2\times L}$ as a vector $\boldsymbol{u} \in \mathbb{R}^p$, where $p = 2L$, the aforementioned equations are cast as a linear system in the form

$$\boldsymbol{A}\boldsymbol{u} = \boldsymbol{b} \tag{14}$$

where $\boldsymbol{A} \in \mathbb{R}^{s\times p}$, $\boldsymbol{b} \in \mathbb{R}^s$ and $s = L + 4$. This system is underdetermined, while $\boldsymbol{A}$ might not have full row rank, i.e., $r_A \leq s$. For instance, dependent rows can appear because some of the coefficients of the polynomials $\hat{\phi}(t)$ set to zero, might be zero anyway, leading to $0 = 0$ equations.

It is now possible to restrict minimization of the objective function $J = J(\boldsymbol{u})$, where $\boldsymbol{u} \in \mathbb{R}^p$, to the set of solutions of Eq. (14) which lie on a lower dimensional space of dimension $p - r_A$. To elaborate further, note that the vector space $U \subseteq \mathbb{R}^p$ of solutions of the system $\boldsymbol{A}\boldsymbol{u} = \boldsymbol{0}$, can be fully described with the aid of a basis $\boldsymbol{S} = [\boldsymbol{s}_1\ \boldsymbol{s}_2\ ...\ \boldsymbol{s}_{p-r_A}]$ for the *nullspace* of $\boldsymbol{A}$ [5] where $\boldsymbol{S} \in \mathbb{R}^{p\times(p-r_A)}$. In this regard, any element $\boldsymbol{u} \in U$ can be represented by an element $\boldsymbol{v} \in V \subseteq \mathbb{R}^{p-r_A}$ as $\boldsymbol{u} = \boldsymbol{S}\boldsymbol{v}$. Then the vector space $U_b \subseteq \mathbb{R}^p$ of solutions of $\boldsymbol{A}\boldsymbol{u} = \boldsymbol{b}$ can be obtained as an affine transformation of U. More specifically, the solutions $\boldsymbol{u} \in U_b$ of Eq. (14) can be represented as $\boldsymbol{u} = \boldsymbol{S}\boldsymbol{v} + \boldsymbol{u}_p$ where $\boldsymbol{u}_p$ is any particular solution of Eq. (14) [5]. It becomes now possible to cast the original constrained optimization problem

$$\underset{\boldsymbol{u}\in\mathbb{R}^p}{\arg\min}\, J(\boldsymbol{u}) \quad \text{subject to} \quad \boldsymbol{A}\boldsymbol{u} = \boldsymbol{b} \tag{15}$$

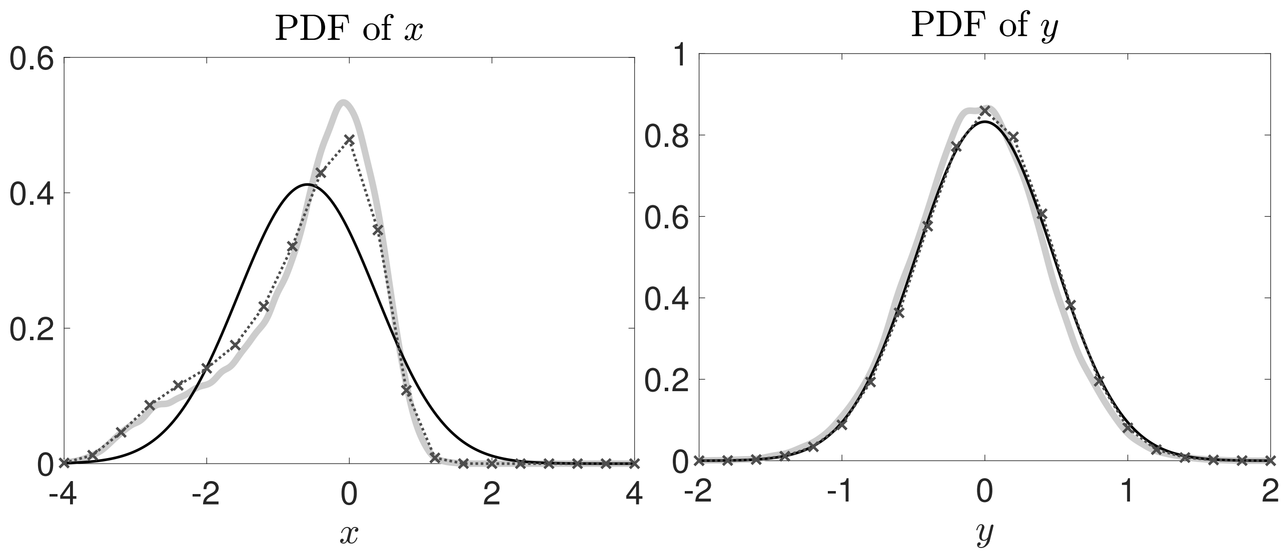

(a) displacement x (b) electrical quantity y

Figure 1: Stationary marginal response PDFs of a nonlinear energy harvester with $\zeta = 0.1$, $\kappa = 0.65$, $\alpha = 0.8$, $\delta = 0.2$ and $S_0 = 0.05$. **Solid gray line:** MC - 50000 realizations, **Solid black line:** Statistical linearization, **Dotted line with "x":** WPI Rayleigh-Ritz-nullspace approach with 7 Legendre polynomials.

into the lower dimensional, unconstrained problem

$$\underset{\boldsymbol{v}\in\mathbb{R}^{p-r_A}}{\arg\min}\, J(\boldsymbol{S}\boldsymbol{v}+\boldsymbol{u}_p) \tag{16}$$

which is solved by applying the optimality conditions $\frac{\partial J(\boldsymbol{S}\boldsymbol{v}+\boldsymbol{u}_p)}{\partial \boldsymbol{v}} = \boldsymbol{0}$. Note that the minimizer $\boldsymbol{u}^*$ of Eq. (15) can be obtained by the minimizer $\boldsymbol{v}^*$ of Eq. (16) as $\boldsymbol{u}^* = \boldsymbol{S}\boldsymbol{v}^* + \boldsymbol{u}_p$.

5. Numerical Examples

To demonstrate the efficiency and accuracy of the proposed technique for analyzing and optimizing energy harvesting systems, a mono-stable asymmetric harvester ($\lambda = 2\sqrt{\delta}, \delta \geq 0$) described by equations (1),(2) is considered in this section.

5.1. Energy harvester stochastic response analysis

Utilizing the herein extended WPI technique of Sec. 4, the stationary joint response PDF $p(x, \dot{x}, y)$ of the nonlinear energy harvester with mono-stable asymmetric potential and parameters $\zeta = 0.1$, $\kappa = 0.65$, $\alpha = 0.8$, $\delta = 0.2$ and $S_0 = 0.05$ is determined. The corresponding marginal PDFs are compared both with pertinent MCS data, and with PDF estimates based on a statistical linearization treatment [10]. The marginal stationary response PDFs of x and y of this energy harvester are shown in Fig. 1, where the WPI based solutions are compared both with pertinent MCS data, and with solutions obtained by applying the statistical linearization method [10].

Clearly, because of the fundamental assumption of a Gaussian response PDF, a standard statistical linearization treatment fails to capture, not only the tails, but also basic features of the response PDFs. Note

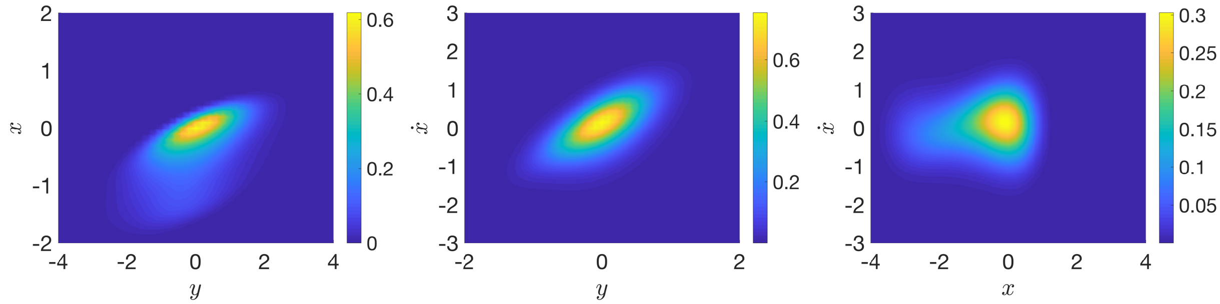

(a) $p(y, x)$ (b) $p(y, \dot{x})$ (c) $p(x, \dot{x})$

Figure 2: Stationary joint response PDFs of a nonlinear energy harvester with $\zeta = 0.1$, $\kappa = 0.65$, $\alpha = 0.8$, $\delta = 0.2$ and $S_0 = 0.05$ obtained by the WPI Rayleigh-Ritz-nullspace approach with 7 Legendre polynomials.

that this inadequacy of statistical linearization becomes significant from an optimization perspective as well, especially when a constrained optimization problem such as the one in Eq. (4) is considered. In particular, if maximizing $\mathbb{E}\{y^2\}$ is the only objective to be taken into account, then statistical linearization could potentially provide with relatively accurate results as suggested by the accuracy degree shown in Fig. 1b related to the PDF of y. However, if a more sophisticated optimization strategy is sought for, such as the one in Eq. (4) with a constraint of the form $P_f = P(|x| > x_{limit}) < \epsilon$, then satisfactory accuracy in estimating the tails of the PDF of x is obviously required. As clearly shown in Fig. 1a, this is achieved by the WPI technique, but not by a statistical linearization treatment.

5.2. Energy harvester optimization

The constrained optimization problem of Eq. (4) is considered in this section. The objective function of this problem, i.e. $P_h(\boldsymbol{z})$ with $\boldsymbol{z} = [\alpha, \delta]^T$, requires the calculation of $\mathbb{E}\{y^2\}$ (see Eq. (3)). Additionally, accounting for the constraint that the probability of failure does not exceed a prescribed threshold ϵ, requires knowledge of the joint response PDF. In this regard, the extended WPI technique developed in Sec. 4 is employed next. The failure scenario $x < x_{limit}$ is taken into account, and the corresponding probability of failure is defined as

$$P_f = P(x < x_{limit}) = \int_{-\infty}^{x_{limit}} p_s(x)\mathrm{d}x \tag{17}$$

where $p_s(x)$ is the stationary marginal PDF of the displacement x. For the solution of the corresponding constrained optimization problem (see Eq. (4)), a penalty approach is utilized. This yields an unconstrained problem with the modified objective function $P_{h,\epsilon}(\boldsymbol{z}) = \mathbb{1}_\epsilon(\boldsymbol{z})P_h(\boldsymbol{z})$ where $\boldsymbol{z} = [\alpha, \delta]^T$ and $\mathbb{1}_\epsilon(\boldsymbol{z})$ is an indicator function equal to 0 if $P_f(\boldsymbol{z}) \geq \epsilon$ and to 1 otherwise.

Taking into account that information regarding the gradient of $P_{h,\epsilon}(\boldsymbol{z})$ is not available in general, and that the modified objective function $P_{h,\epsilon}(\boldsymbol{z})$ is discontinuous, the gradient-free Generalized Pattern Search (GPS) optimization algorithm is utilized next [11]. First, the performance of the GPS algorithm is assessed by comparisons with brute-force full grid evaluations of the objective function $P_{h,\epsilon}(\boldsymbol{z})$ by relying on statistical linearization. In this regard, a full grid computation of $P^{SL}_{h,\epsilon}(\alpha, \delta)$ in the interval $\{\alpha, \delta\} \subset [0.5, 1.5] \times [0, 0.5]$

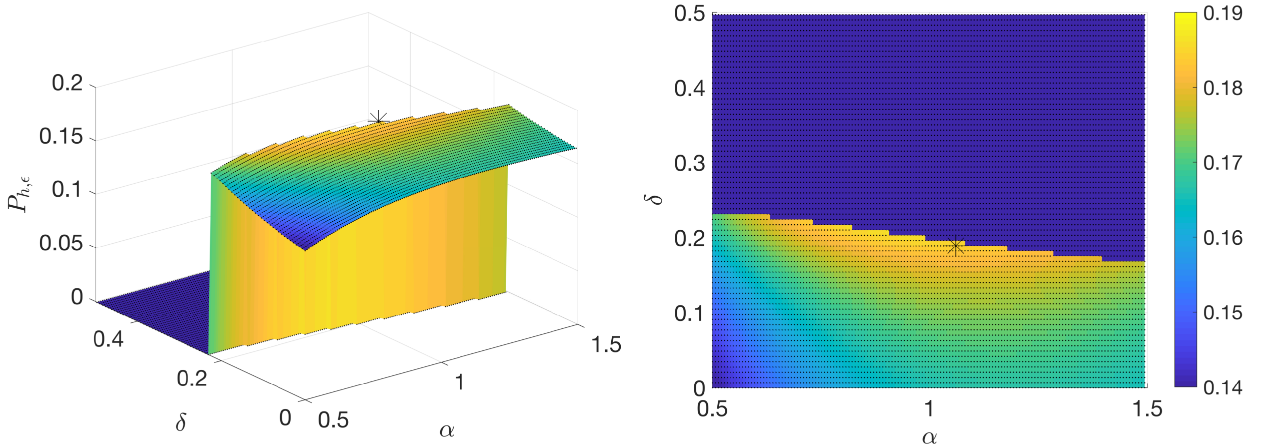

Figure 3: Stationary mean harvested power $P_{h,\epsilon}$ obtained by statistical linearization with constraint of the form of Eq. (17), and parameters $x_{limit} = -3.0$ and $\epsilon = 10^{-2}$. Full grid computation with mesh size 0.007 required 10296 objective function evaluations: $(\alpha_{opt}, \delta_{opt}) = (1.0600, 0.1890)$, $P^{SL}_{h,\epsilon}(\alpha_{opt}, \delta_{opt}) = 0.1850$ and $P_f(\alpha_{opt}, \delta_{opt}) = 0.009864$.

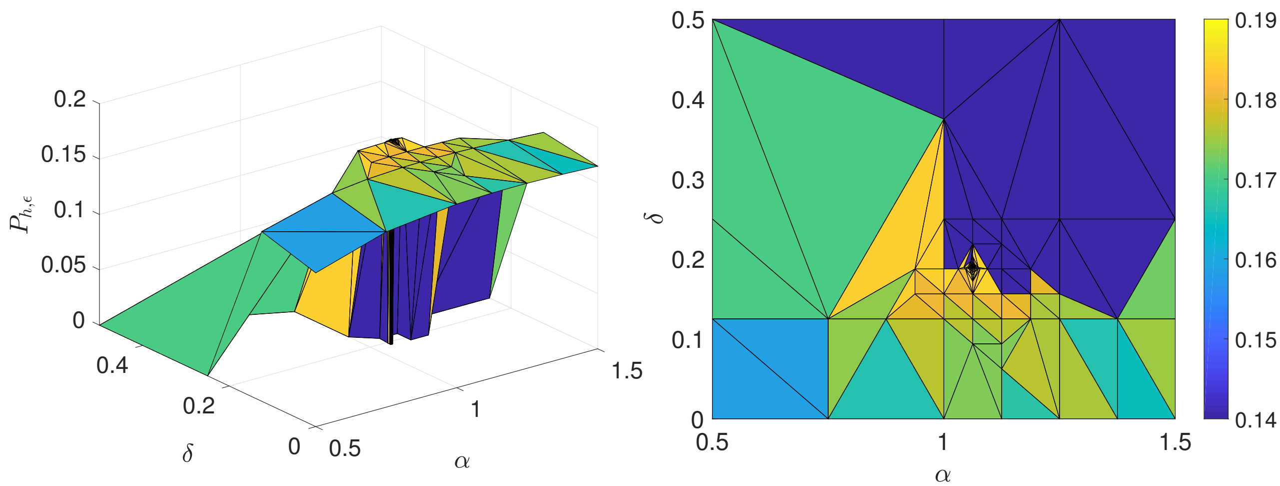

Figure 4: Stationary mean harvested power $P_{h,\epsilon}$ obtained by statistical linearization with constraint of the form of Eq. (17), and parameters $x_{limit} = -3.0$ and $\epsilon = 10^{-2}$. GPS optimization required 164 objective function evaluations to converge: $(\alpha_{opt}, \delta_{opt}) = (1.0580, 0.1907)$, $P^{SL}_{h,\epsilon}(\alpha_{opt}, \delta_{opt}) = 0.1853$ and $P_f(\alpha_{opt}, \delta_{opt}) = 0.009987$.

with a mesh size of 0.007 and parameter values $\zeta = 0.1$, $\kappa = 0.65$ and $S_0 = 0.05$, is presented in Fig. 3, with the constraint $P_f = P(x < -3.0) \leq 10^{-2}$, showing the existence of a global optimum point. Next, the GPS algorithm is employed to solve the same problem and the results presented in Fig. 4 exhibit practically the same accuracy as the full grid computation. Note, however, that approximately only $\sim 0.5\%$ of the objective function evaluations used in the full grid computation are required by the GPS algorithm, rendering the overall optimization scheme computationally efficient.

Finally, the optimization results obtained by the WPI technique are shown in Fig. 5, revealing the significant but anticipated difference between the WPI and the linearization based optimal designs. This is attributed primarily to the incapability of statistical linearization to capture accurately the tails of the response PDF, which are related to the constraint of Eq. (17). The above argument is corroborated further by Table 1,

Constraint: $P_f = P(x < -3.0) \leq 10^{-2}$		
	WPI optimum $(\alpha, \delta) = (0.9874, 0.0625)$	**Stat. Lin. optimum** $(\alpha, \delta) = (1.0580, 0.1907)$
P_h	0.16886	0.18530
P_f	0.00998	0.00999
MCS		
P_h	0.17021	0.17731
P_f	0.00932	0.03664

Table 1: Assessment of the WPI and statistical linearization based optima using MCS with 50000 realizations.

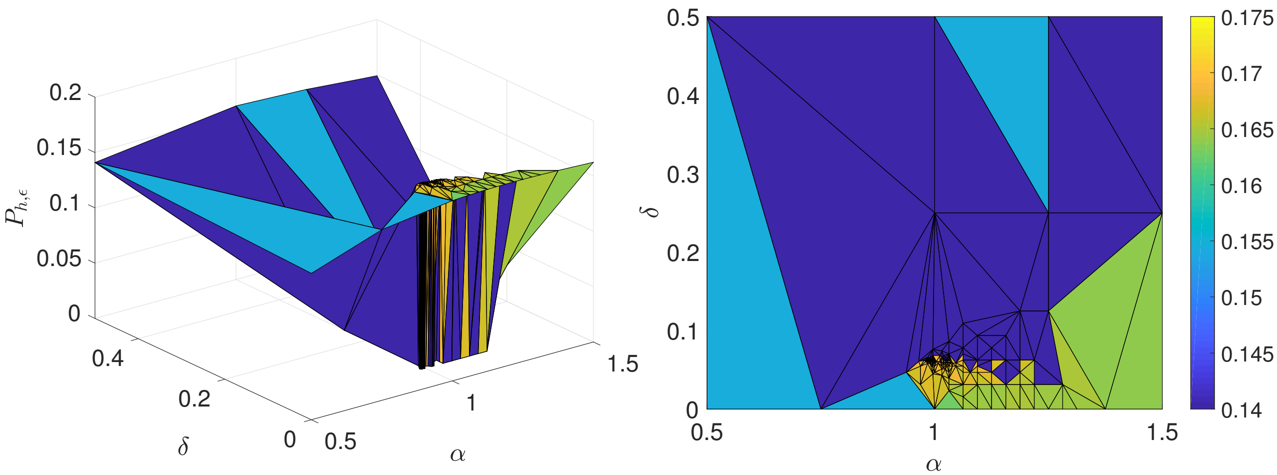

Figure 5: Stationary mean harvested power $P_{h,\epsilon}$ obtained by WPI with constraint of the form of Eq. (17), and parameters $x_{limit} = -3.0$ and $\epsilon = 10^{-2}$. GPS optimization required 144 objective function evaluations to converge: $(\alpha_{opt}, \delta_{opt}) = (0.9874, 0.0625)$, $P_{h,\epsilon}^{WPI}(\alpha_{opt}, \delta_{opt}) = 0.1689$ and $P_f(\alpha_{opt}, \delta_{opt}) = 0.009981$.

where the WPI and linearization based optimal designs are assessed by using MCS. In particular, the WPI based optimum design yields a probability of failure of 0.00932, which is very close to the prescribed threshold (10^{-2}). On the other hand, the linearization based optimum design yields a $P_f = 0.03664$ that is significantly larger than 10^{-2}, and thus violates the imposed constraint.

6. Concluding remarks

A methodology based on the WPI technique has been developed for determining the response of a class of nonlinear electromechanical energy harvesters subject to Gaussian white noise excitation. In this regard, the WPI technique [3, 4] has been extended to account for a singular diffusion matrix present in the governing equations. Specifically, treating the coupled electromechanical equations as an "underdetermined" SDE in conjunction with a constraint equation has yielded a constrained variational problem, solved by utilizing the nullspace of the constraint equation. It has been shown that the WPI technique exhibits satisfactory accuracy in determining the joint response PDF as compared with pertinent MCS data, and significantly outperforms an alternative statistical linearization treatment. Next, the herein extended WPI technique has been coupled with an appropriate optimization algorithm (GPS) for determining optimal parameters for the energy harvester with constraints referring to a failure probability. For such cases, where relatively high accuracy in determining the response PDF tails is required, optimization based on statistical linearization yields, in general, either sub-optimal solutions or solutions that violate the constraint.

References

[1] M. F. Daqaq, R. Masana, A. Erturk, D. D. Quinn, On the role of nonlinearities in vibratory energy harvesting: a critical review and discussion, Applied Mechanics Reviews 66 (4) (2014) 040801.

[2] S. Adhikari, M. Friswell, D. Inman, Piezoelectric energy harvesting from broadband random vibrations, Smart Materials and Structures 18 (11) (2009) 115005.

[3] I. Kougioumtzoglou, P. Spanos, An analytical Wiener path integral technique for non-stationary response determination of nonlinear oscillators, Probabilistic Engineering Mechanics 28 (2012) 125–131.

[4] I. A. Kougioumtzoglou, P. D. Spanos, Nonstationary stochastic response determination of nonlinear systems: A Wiener path integral formalism, Journal of Engineering Mechanics 140 (9) (2014) 04014064.

[5] G. Strang, Linear Algebra and Its Applications, 4th Edition, Thomson Higher Education, Belmont, CA, 2006.

[6] Q. He, M. F. Daqaq, Electric load optimization of a nonlinear mono-stable duffing harvester excited by white noise, Meccanica 51 (5) (2016) 1027–1039.

[7] O. C. Zienkiewicz, Finite elements and approximation, Dover Publications, Mineola, N.Y, 2006.

[8] I. A. Kougioumtzoglou, A Wiener Path Integral Solution Treatment and Effective Material Properties of a Class of One-Dimensional Stochastic Mechanics Problems, Journal of Engineering Mechanics 143 (6) (2017) 04017014.

[9] L. D. Elsgolc, Calculus of variations, Dover Publications, Mineola, N.Y, 2007.

[10] J. B. Roberts, P. D. Spanos, Random Vibration and Statistical Linearization (Dover Civil and Mechanical Engineering), Dover Publications, Mineola, NY, 2003.

[11] V. Torczon, On the convergence of pattern search algorithms, SIAM Journal on optimization 7 (1) (1997) 1–25.